Correlating Structure with Function in Thermally Annealed PCDTBT:$PC_{70}BM$ Photovoltaic Blends

Tao Wang, Andrew J. Pearson, Alan D. F. Dunbar, Paul A. Staniec, Darren C. Watters, Hunan Yi, Anthony J. Ryan, Richard A. L. Jones, Ahmed Iraqi, and David G. Lidzey**

A range of optical probes are used to study the nanoscale-structure and electronic-functionality of a photovoltaic-applicable blend of the carbazole co-polymer poly[*N*-9′-heptadecanyl-2,7-carbazole-alt-5,5-(4′,7′-di-2-thienyl-2′,1′,3′-benzothiadiazole) (PCDTBT) and the electronic accepting fullerene derivative (6,6)-phenyl C_{70}-butyric acid methyl ester ($PC_{70}BM$). In particular, it is shown that the glass transition temperature of a PCDTBT:$PC_{70}BM$ blend thin-film is not sensitive to the relative blend-ratio or film thickness (at 1:4 blending ratio), but is sensitive to casting solvent and the type of substrate on which it is deposited. It is found that the glass transition temperature of the blend reduces on annealing; an observation consistent with disruption of π–π stacking between PCDTBT molecules. Reduced π–π stacking is correlated with reduced hole-mobility in thermally annealed films. It is suggested that this explains the failure of such annealing protocols to substantially improve device-efficiency. The annealing studies demonstrate that the blend only undergoes coarse phase-separation when annealed at or above 155 °C, suggesting a promising degree of morphological stability of PCDTBT:$PC_{70}BM$ blends.

1. Introduction

Growing concerns about fuel security and global warming have made the development and use of devices that harvest energy from sunlight a priority research area. Organic photovoltaics (OPVs) are one class of solar-energy conversion device, offering the advantages of low cost, light-weight, solution-processability and mechanical-flexibility over existing photovoltaic technologies.[1–3] Polymer–fullerene bulk heterojunction (BHJ) OPVs now demonstrate power conversion efficiencies (PCE) above 8% when measured under laboratory conditions.[4]

Achieving power conversion efficiencies and device lifetimes in OPVs appropriate for commercial viability requires the efficiency and stability of the photocurrent generation process to be maximized. In order to do this, it is necessary to control the nanoscale morphology of a blend thin-film when fabricated into a solar cell device, as this impacts on the efficiency of charge generation, extraction and operational-stability. A number of studies have addressed this issue using a photovoltaic-active blend of the polymer poly(3-hexylthiophene) (P3HT) and the fullerene acceptor (6,6)-phenyl C61-butyric acid methyl ester (PCBM.) When blended together and processed using appropriate protocols, these materials undergo both phase-separation and crystallization, providing a useful test-bed to explore the role of nanoscale morphology on the optoelectronic characteristics of the blend.[5–8] We have previously demonstrated that after casting a thin-film from a P3HT:PCBM blend solution, P3HT can undergo partial crystallization into ordered lamellae.[9] This limited phase separation between components can allow for the formation of a bi-continuous network within the film. Such films are typically spin-cast from relatively volatile solvents, with the fast drying-time of the film resulting in a nanoscale morphology that is not well suited for photocurrent generation and charge-extraction. To address this issue, a number of techniques have been used to modify film structure. These include the use of solvent additives to control the drying process,[10] and post-deposition techniques such as thermal annealing[5,11] and solvent annealing[12,13] to increase the relative crystallinity of the P3HT and PCBM phases as well as to control the vertical composition of the active layer.[14] As a result, such processes can enhance optical absorption,[15] charge separation[16,17] charge transport[18] which thus facilitates charge extraction.

The polymer poly[N-9′-heptadecanyl-2,7-carbazole-alt-5,5-(4′,7′-di-2-thienyl-2′,1′,3′-benzothiadiazole) (PCDTBT) is one of a new generation of polymers that have been designed for OPV applications. When blended with a suitable electron-acceptor such as $PC_{70}BM$ and fabricated into an OPV device, power con-

Dr. T. Wang, A. J. Pearson, D. C. Watters,
Prof. R. A. L. Jones, Prof. D. G. Lidzey
Department of Physics and Astronomy
University of Sheffield
Sheffield, S3 7RH, UK
E-mail: taowang@sheffield.ac.uk; d.g.lidzey@sheffield.ac.uk
Dr. A. D. F. Dunbar
Department of Chemical and Biological Engineering
The University of Sheffield
Sir Robert Hadfield Building
Mappin St, Sheffield S1 3JD, UK
Dr. P. A. Staniec
Diamond Light Source Ltd, Diamond House
Harwell Science and Innovation Campus
Didcot, Oxfordshire OX11 0DE, UK
Dr. H. Yi, Dr. A. Iraqi, Prof. A. J. Ryan
Department of Chemistry
University of Sheffield
Sheffield, S3 7RH, UK

DOI: 10.1002/adfm.201102510

version efficiencies of between 6 and 7% can be achieved.[19,20] Here, the improvement in PCE compared to an OPV based on a P3HT:PCBM blend is primarily due to a closer alignment of molecular orbital energy levels between donor and acceptor, resulting in a higher open-circuit voltage (V_{oc}). The lower optical band-gap of PCDTBT (1.8 eV) compared to P3HT (1.9 eV) also helps to improve the efficiency by which sunlight is harvested as it provides increased absorption at longer wavelengths.

While the polymer P3HT is a semi-crystalline material, PCDTBT is a largely amorphous polymer and is characterized by weak intermolecular interaction resulting from π–π stacking between the conjugated back-bones.[21,22] The phase behavior, optical and electrical properties of PCDTBT and its miscibility with $PC_{70}BM$ have not been systemically investigated, particularly in a thin film geometry that is representative of a solar cell device. Consequently the suitability or applicability of a variety of post deposition techniques previously used to improve the efficiency of P3HT-based OPVs are not well understood. We address this by using spectroscopic ellipsometry (SE)[11] to characterize the thermal transitions of a series of PCDTBT:$PC_{70}BM$ blend films, with our studies focusing on the glass transition temperature (T_g) of PCDTBT component. We complement this using ex-situ grazing incidence wide-angle X-ray scattering (GIWAXS), together with measurements of UV-Vis absorption and photoluminescence emission and hole-carrier mobility (via space-charge limited conduction techniques). We show that upon mixing $PC_{70}BM$ with PCDTBT, polymer photoluminescence is very efficiently quenched and that hole-mobility is enhanced; an effect we attribute to the amorphous nature of PCDTBT. Furthermore we show that by annealing a PCDTBT:$PC_{70}BM$ blend above its T_g, the degree of average structural order within the film is reduced; an effect that results in reduced charge mobility in OPVs having lower power conversion efficiency. We conclude that thermal annealing protocols commonly used to improve P3HT:PCBM blend OPVs are unlikely to improve the efficiency of PCDTBT:$PC_{70}BM$ OPV devices by improving the average state of order of the polymer component. Importantly however, we show that the PCDTBT:$PC_{70}BM$ blend does not undergo coarse phase separation when annealed at a temperature below 155 °C; a result that suggests that its morphology is more stable than a comparable P3HT:PCBM blend. Such thermal stability is a promising advantage of this family of materials.

2. Results and Discussion

We have used spectroscopic ellipsometry to determine the glass transition temperature of a PCDTBT:$PC_{70}BM$ blend film cast under a series of different initial conditions. In **Figures 1**a,b and c, we plot the ellipsometric parameter Ψ recorded during first heating of a PCDTBT:$PC_{70}BM$ (1:4 wt%) thin-film blend, cast from chloroform (CF), chlorobenzene (CB) or 1,2-dichlorobenzene (DCB) respectively. Here, the PCDTBT polymer used has an M_w of 29.3 kDa. Thermal transitions are identified by the intersection of straight-line fits to the linear sections of a Ψ vs T plot. We have previously used this technique to study phase-transitions in thin-film blends of P3HT and PCBM[11,23] with other authors applying it to the study of the saturated polymer PS[24] and the conjugated polymer F8TBT.[25] As we describe below, the possible thermal processes within such films can be manifested by an increase or a decrease of $d\Psi/dt$. In Figures 1a, b and c, we observe a number of different transitions. We first concentrate on the reduction in $d\Psi/dt$ of the blend films that occur when the films are heated to 65 °C, 135 °C and 175 °C respectively. We found that these temperatures are close to the boiling points of the casting solvents CF, CB and DCB that occur at 62 °C, 132 °C and 180 °C respectively as reported by the supplier Sigma Aldrich. The coincidence between these temperatures and the apparent reduction in the thermal expansion rate of the films suggests we are observing the evaporation of residual solvent from the film once the annealing temperature exceeds T_e (with T_e defined as the temperature at which the residual solvent begins to evaporate rapidly from the blend thin films upon heating).

The presence of trapped solvent within a film results from the fact that during solution casting, the glass transition temperature (T_g) of film is initially reduced as the solvent acts as a plasticizer. When the solvent evaporates as the film dries, its T_g increases and once it exceeds the (ambient) casting temperature, evaporation will be opposed by the very slow volume-relaxation of the glassy film,[26] with a small amount of solvent being trapped at the point at which the film vitrifies.[11,27] The

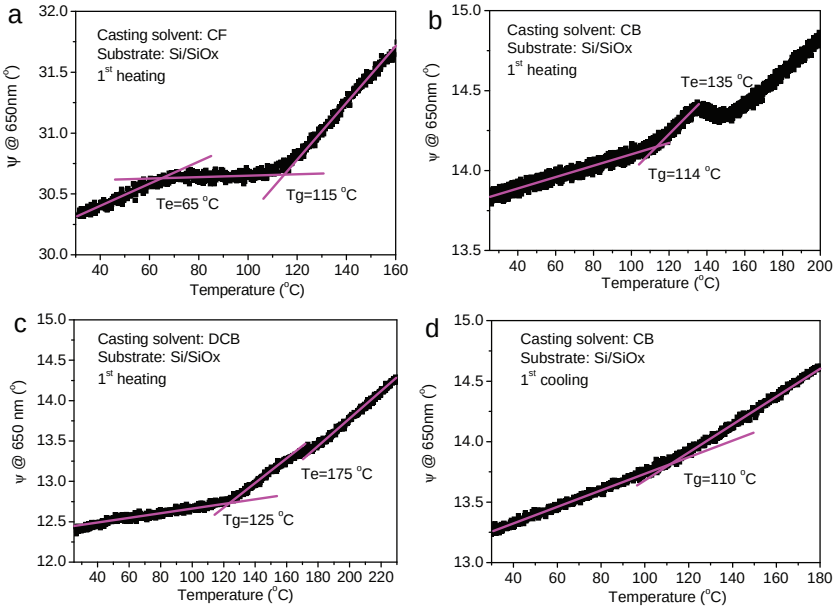

Figure 1. The ellipsometric parameter Ψ vs. temperature recorded during the first heating cycle of a PCDTBT:$PC_{70}BM$ thin film spin-cast from a) CF, b) CB and C) DCB. The trapped CF, CB and DCB in the solid films evaporate at a temperature around the boiling points of the respective casting solvent. d) The ellipsometric parameter Ψ vs. temperature recorded during the first cooling cycle of a PCDTBT:$PC_{70}BM$ thin film, with the intersection of the slopes of the glassy and rubbery states defining the T_g of the film. Note the PCDTBT material used in Figure 1 has an M_w of 29.3 kDa.

presence of trapped solvent within a blend thin-film can be evidenced by monitoring changes in film thickness during heating. This heating process will result in an expansion in the volume of a solid film, however the loss of solvent will result in an apparent contraction in film thickness as it is heated above T_e as shown in Figure 1(a), (b) and (c).[11] It is clear that the reduction in $d\Psi/dt$ observed in a DCB-cast film annealed above 175 °C (see Figure 1c) is not as large as that occurs in a CB cast film when heated above 135 °C (see Figure 1b). We have previously shown[11] that trapped solvent can evaporate relatively slowly when a film is heated above its T_g but below the boiling point of the casting solvent. As we show below, the T_g of PCDTBT in the blend is over 100 °C and thus the high T_e of DCB results in a DCB-cast film being held above T_g but below T_e for a longer period of time than occurs for an equivalent CB-cast film. Because of this, it is likely that relatively more solvent will have been released in a DCB-cast film before T_e is reached; an explanation consistent with the relatively smaller contraction observed when such films are heated past 175 °C.

Figure 1d shows the first cooling cycle of a PCDTBT:$PC_{70}BM$ 1:4 wt% blend film cast from CB. Here a single thermal transition is observed at 110 °C, that we identify (following a well-accepted procedure[24]) as being the film T_g. Here, all solvent has been removed from the film during the initial heating process and thus the observed contraction corresponds to a transition from a rubbery to a glassy state. We can use this identification to rationalize the other transitions observed in Figures 1a,b and c. Here, a thermal transition is apparent at 115, 114 and 125 °C respectively, which in all cases we associate with T_g. In the following sections, we will discuss the apparent deviations of T_g in films cast using different solvents, blend compositions and on different substrates.

In **Figures 2**a to f we plot the thermal expansivity on heating or cooling of a PCDTBT:$PC_{70}BM$ blend film that was cast or measured under a number of different conditions. Here the PCDTBT polymer has an M_w of 32.6 kDa. Specifically, part (a) shows a PCDTBT:$PC_{70}BM$ blend film (1:4 wt%) cast from DCB onto a silicon/native oxide (Si/SiOx) substrate as it is heated and then cooled. Part (b) shows film contraction during 1st cooling when a blend film (1:1 wt%) cast either on a PEDOT:PSS or a Si/SiOx substrate from a DCB solution. Part (c) shows the effect of film thickness on contraction whilst part (d) similarly shows the effect of the relative composition ratio of PCDTBT and $PC_{70}BM$ in the thin film blend (when cast from CF on a Si/SiOx substrate) with measurements recorded during film cooling (i.e. containing no remaining trapped solvent). In each case we identify and state the measured T_g in the figure. In parts (e) and (f), we plot T_g as a function of $PC_{70}BM$ concentration on different substrates (part (e)) and from different casting solvents (part (f)).

It can be seen in Figure 2a that the T_g of the film is apparently different if it is measured during the heating or cooling cycle. Specifically, we see an apparent glass-transition at 145 °C when the film is first heated; a value that reduces to 129 °C as the film is then cooled. In Figure 1, we demonstrated the existence of residual casting solvent trapped inside of the film. In the data presented in Figure 2a, the film was cast from DCB (T_e ~175 °C), and thus the heating cycle is anticipated to have removed all the solvent from the film. It is clear however that the heating cycle reduces the film T_g. This is a surprising result, as organic solvents generally act as a plasticizer, decreasing the T_g of a polymer film compared to its non-solvent counterpart. This result appears quite general and independent of casting solvent, substrate or blend composition as shown in Figure 2e and f. We speculate, therefore, that the heating cycle reduces the average degree of intermolecular interaction (π–π stacking) in the blend thin-films; an effect that results in a reduction of T_g.

We base this conclusion on the results of our GIWAXS study on PCDTBT. Here, we found that intermolecular interactions between polymer chains are reduced after the polymer film is annealed at a temperature in excess of ~100 °C. We quantify this in **Figure 3** by plotting the π–π stacking coherence-length of a PCDTBT thin film as a function of annealing temperature. This data is extracted from the GIWAXS plots shown in Figure S1 (Supporting Information), with stacking coherence length calculated using $L_{co} = 2\pi/\Delta q$, where Δq is the full width at half maximum of the scattering peaking at $q = 1.57$ Å^{-1}. We find that side-chain order of PCDTBT increases upon thermal annealing at a temperature ≥ 130 °C, as evidenced by the appearance of a 2nd order side-chain crystalline diffraction peak at $q = 0.63$ A^{-1} in the out of plane direction (see Figure S1, Supporting Information). Our results and conclusions are in good agreement with results of a similar study published elsewhere,[22] suggesting that the increased side-chain order during thermal treatment reduces π–π stacking. Note however the molecular weight (M_w) of the PCDTBT used in this study is significantly smaller than that used in Ref 22 (32.6 kDa compared to 120 kDa) and thus the coherence length of the π–π stacking determined in this work is smaller. We believe that this disruption in π–π stacking on annealing cannot be simply explained by the changes in the local concentration of the PCBM, as the results presented in Figure 2e and f suggest that the film T_g is almost constant over most of the range of blend concentrations studied. This demonstrates that PCBM does not significantly change the thermal properties of PCDTBT.

In Figure 2b we compare the thermal expansion (and thus T_g) of a blend film (1:1 wt%) cast from DCB onto a Si/SiOx surface with an otherwise identical film cast onto a film of the conductive polymer PEDOT:PSS; a material frequently used to aid the extraction of holes from an OPV. We also summarize T_g for a range of different blend compositions and casting solvents for both heating and cooling cycles in Figure 2e and f. It can be seen that the T_g of the blend cast on a PEDOT:PSS substrate is approximately 5 to 10 °C lower than when cast on Si/SiOx. This suggests that π–π stacking of PCDTBT is more efficiently stabilized on a Si/SiOx surface compared to PEDOT:PSS. Indeed, we have found that π–π stacking can be stabilized at the buried PCDTBT-Si/SiOx substrate interface.[28] The apparently improved intermixing of PCDTBT with PEDOT:PSS compared to Si/SiOx might account for this. We emphasize that the data presented in Figure 2b has been determined during a cooling cycle, and thus any solvent has been removed and should not impact on the different T_g of the blend deposited on different substrates. We find that the T_g of the blend cast from DCB is higher than a comparable film cast from CF, suggesting a greater degree of π–π stacking. We speculate that as PCDTBT is more soluble in DCB than in CF, the polymer chains are more likely to adopt an extended conformation in solution. As the solution is cast into a thin film, the polymer chains are more likely to retain such an "open" configuration, resulting in a greater degree of π–π stacking.

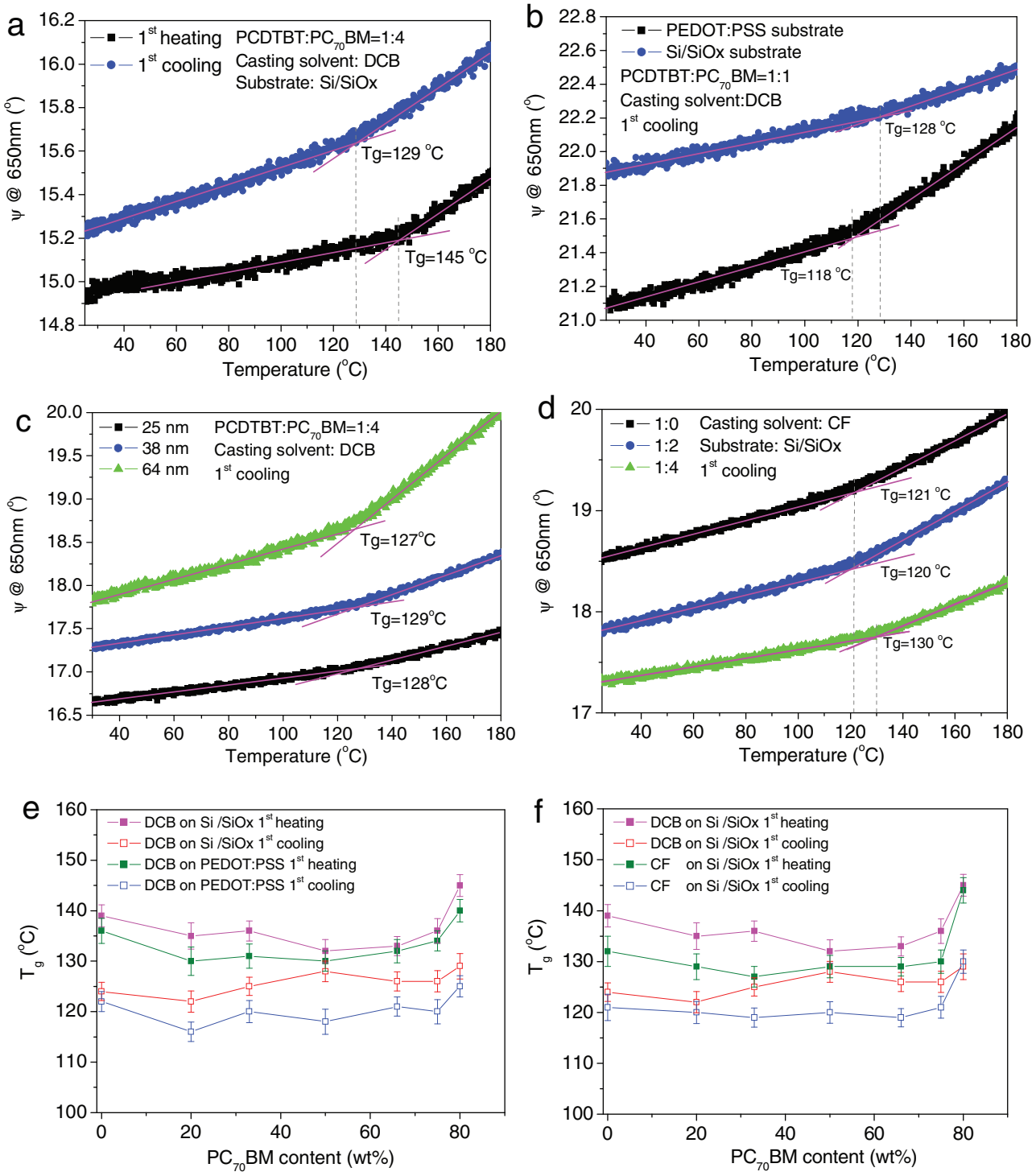

Figure 2. a) The ellipsometric parameter Ψ vs. temperature recorded during the first heating cycle and cooling cycle of a PCDTBT:PC_{70}BM blend thin film spin-cast from DCB. b) Ψ vs. temperature recorded during a cooling cycle for a blend film (1:1 wt%) on a Si/SiOx and a PEDOT:PSS substrate. c) Cooling cycles for a PCDTBT:PC_{70}BM blend in which the thickness of the film is varied. d) Cooling cycles for a PCDTBT:PC_{70}BM blend film in which the ratio between the PCDTBT and PC_{70}BM has been varied. In all cases, the temperature corresponding to T_g has been identified. The curves in (a) to (d) have been vertically shifted for clarity. In (e) and (f) we summarise T_g for a series of blend films having different blend ratios, when cast from DCB on Si/SiOx and PEDOT:PSS (e), and from DCB and CF on Si/SiOx (f). In all cases, the M_w of the PCDTBT is 32.6 kDa.

It can be seen in Figure 2c that for the 1:4 wt% blend film, T_g has a weak (or negligible) dependence of film thickness, with T_g variations falling within measured uncertainty as the film thickness is varied between 25 and 64 nm. We note that anomalous T_g behavior has been previously observed in polymer/nanoparticle composite systems,[29] with such composites typically

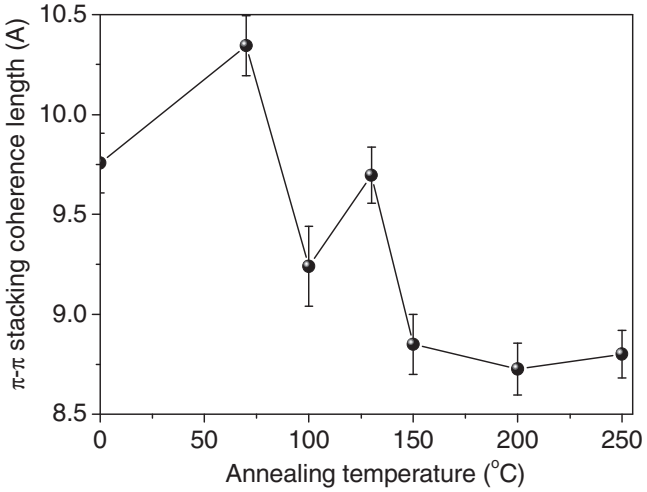

Figure 3. The π–π stacking coherence length of PCDTBT in a thin film as a function of annealing temperature as measured by GIWAXS.

containing a nanoparticle loading of a few percent by weight. In our experiments however, we explore a considerably higher blending ratio. It is known that PCDTBT and $PC_{70}BM$ undergo efficient intermixing,[30] and thus we speculate that the confinement resulting from molecular mixing is larger than free-surface effects that often reduce T_g.[31] If our speculation is correct, it would suggest therefore the absence of a mobile (liquid-like) surface-layer in a PCDTBT:$PC_{70}BM$ blend film as has been observed in a number of other polymer systems.[24,29,31]

Despite the difference in T_g observed on the different substrates and when cast from different solvents, Figures 2e and f indicate that T_g is relatively insensitive to relative film composition, being approximately constant for $PC_{70}BM$ loadings of up to 75 wt%. A similar result has also been observed in thin films of a structurally similar conjugated polymer (F8TBT) when blended with PCBM.[25] However, once the $PC_{70}BM$ concentration is increased to 80 wt%, a small (5 °C) increase in T_g is observed. For completeness, we have also explored the effect of the molecular weight of PCDTBT on its T_g. Here, we have measured thin films of the pure polymer (with all films having a thickness of 30 ± 2 nm) cast from CF on a Si/SiOx substrate determined during the 1st cooling cycle. As shown in **Figure 4**a, we determine a T_g of 100, 110 and 121°C for PCDTBT having an M_w of 22.5 kDa, 29.3 kDa and 32.6 kDa respectively. Clearly the significant influence of M_w on T_g suggests that the polymers studied here have a M_w below the entanglement molecular weight for PCDTBT.

We now explore the thermal transitions of $PC_{70}BM$. Figure 4b shows the thermal expansion of a 120 nm thick-film of pure $PC_{70}BM$ cast from CF onto a Si/SiOx substrate. It can be seen that two transitions are detectable during the first heating cycle occurring at 110 °C and 155 °C. The lower temperature transition at 110 °C is non-reversible. As PCBM is known to be hydroscopic, this feature may originate from the removal of trapped moisture.[32] The higher temperature thermal transition (155 °C) is however reversible, and is observed during first heating, first cooling and a second heating cycle. The melting temperature of $PC_{70}BM$ is known to be above 250 °C,[32] suggesting the thermal transition at 155 °C is a solid-solid transition. Note that a transition at around 155 °C has also been observed in P3HT:PCBM blend films using dynamic mechanical thermal analysis.[32] In Figure 2 it can be seen that we do not observe a transition at 155 °C in any of the annealing experiments performed on the blends. The apparent absence of this transition suggests that PCDTBT and $PC_{70}BM$ are intimately mixed in the as-cast films. Note however, at high $PC_{70}BM$ loadings, (e.g., 80 wt%) $PC_{70}BM$ nanodomains are expected to form which facilitate efficient electron transport in optimized PCDTBT:$PC_{70}BM$ OPVs.[19] It appears however that such nanodomains are sufficiently small that the solid-solid transition at 155 °C is suppressed. Nevertheless, in the following sections we demonstrate that when the annealing temperature of the blend exceeds 155 °C during a (long) isothermal thermal soak, phase separation and crystallization of $PC_{70}BM$ can occur.

Figure 5a shows the change in thickness of a PCDTBT:$PC_{70}BM$ 1:4 wt% blend film (cast from CF) determined using spectroscopic ellipsometry as a function of time during a thermal ramp and an isothermal soak. Here, we calculated the normalized change in film thickness (h) using $(h - h_0)/h_0$, where h_0 is the thickness of the film before heating. Data is plotted for three different isothermal soak temperatures (130, 150 and 155 °C), with part (a) focusing on the first 300 s of the experiment, whilst part (b) plotting data recorded over the duration of the entire experiment (3750 s). Here, the return to room temperature can be seen at the end of the experiment. It can be seen in part (a) that the film undergoes a contraction in thickness when it is heated to around 65 °C; a temperature coincident with the boiling point of CF. During the isothermal soak, we evidence a slow reduction in the overall thickness of the film. It is known that during a spin-casting (or quenching) process, a large free volume will be "frozen in" to a vitrified polymer thin film.[33–35] Upon heating, the amorphous PCDTBT molecules rearrange to reduce the relative non-equilibrium conformations within the film and results in an overall reduction in free volume of the film. This process usually

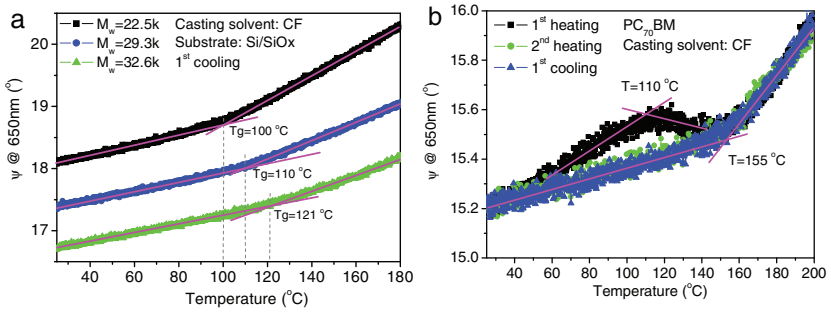

Figure 4. a) The ellipsometric parameter Ψ vs. temperature recorded during the 1st cooling cycle of a series of PCDTBT thin films having different molecular weights spin-cast from CF. In each case, the film thickness was approximately 30 nm. Films were cast on a Si/SiOx substrate, with the T_g transition marked in the figure. b) The heating cycle, cooling cycle and second heating cycle of a $PC_{70}BM$ film (120 nm thick). The transition at 155 °C is identified. The loss of adsorbed moisture is observed at around 110 °C.

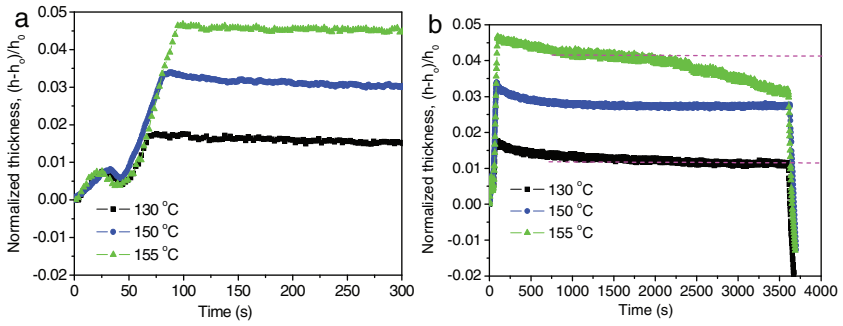

Figure 5. a) The thermal expansion of PCDTBT:$PC_{70}BM$ (1:4) film during heating and isothermal annealing. Here, films were annealed at 130, 150 or 155 °C. Data is plotted for the first 300 s of the experiment. b) The same thermal expansion data as presented in (a), however the data is plotted over the entire course of the experiment lasting over 3,750 s. Here, the cooling and contraction of the films can be seen at the end of the experiment.

takes a long time for the system to finally reach an equilibrium state.[33–35] We find that the reduction of film thickness is initially rapid, but then slows with a pseudo-plateau being reached. We find that the time required to reach this pseudo-plateau is dependent on the annealing temperature and occurs more rapidly as the temperature is raised. We have previously observed this process in P3HT-PCBM blends,[11] and found the volume relaxation process proceeds by P3HT undergoing both amorphous-to-crystalline and amorphous-to-amorphous transitions. Note that whilst the annealing process will reduce the relative fraction of molecules whose conformation is in a non-equilibrium state, the molecular morphology of the photovoltaic blend film does not necessarily reach an equilibrium conformation by the end of the thermal annealing "soak" that we explore here.

Turning to Figure 5b, it can be seen that when the PCDTBT:$PC_{70}BM$ blend film is annealed at 130 or 150 °C, the pseudo-plateau that is established exists for the entire duration of the annealing process. In contrast, however, when a film is annealed at a temperature >155 °C, there is an additional reduction in film thickness that occurs at a time t > 2,100s. Our measurements on P3HT:PCBM blends demonstrated that this reduction in thickness was correlated with the coarse phase-separation of P3HT and PCBM.[11] In particular, we argued that the depletion of material from the bulk combined with the formation of micron-sized crystallites reduces the average film thickness and increases film roughness. We evidence a very similar process here. **Figure 6**a presents an optical microscopy image of an as-cast PCDTBT:$PC_{70}BM$ blend film, whilst parts (b), (c) and (d) show a similar film annealed at 130, 155 and 200 °C for one hour respectively. It can be seen in Figure 6b that when films have been annealed at 130 °C and cooled to room-temperature, no apparent structure is observed (although structure may well be present at a length-scale below the resolution of the optical microscope). When the film is annealed at 155 °C (Figure 6c), structures (which we assume to be $PC_{70}BM$ crystallites) are visible. Such structures become significantly coarser when films are annealed at 200 °C (see Figure 6d). Interestingly, when we anneal a blend film at 155 °C for 30 minutes (image not shown) no $PC_{70}BM$ crystallites can be seen; an observation also supported by our GIWAXS measurements (vide infra). The correlation of the appearance of crystallization in a film annealed at 155 °C for 35 minutes with the reduction in thickness shown in Figure 5b that occurs simultaneously suggests that at this point the $PC_{70}BM$ undergoes micrometer-scale phase-separation. We note that the onset temperature for this process is coincident with a solid-solid transition at 155 °C in $PC_{70}BM$ determined via ellipsometry as shown in Figure 4b. This solid-solid transition is likely to be the cold-crystallization of $PC_{70}BM$ in the blends, indicating that cold-crystallization of $PC_{70}BM$ apparently drives phase separation in the blend film.

We have previously shown[11] that when a P3HT:PCBM blend (60:40 wt%) is annealed at 150 °C, coarse phase-separation and crystallization of PCBM was observed after t = 1000 s. Here, our films contain a much higher fraction of fullerene (80 wt%), however coarse phase separation only occurs after a much longer annealing (2100 s) at a similar temperature. A comparison plot is presented in the supporting information, Figure S2, Supporting Information. We believe that this delay in phase-separation and crystallization is a further manifestation of the improved molecular mixing of $PC_{70}BM$ with PCDTBT.

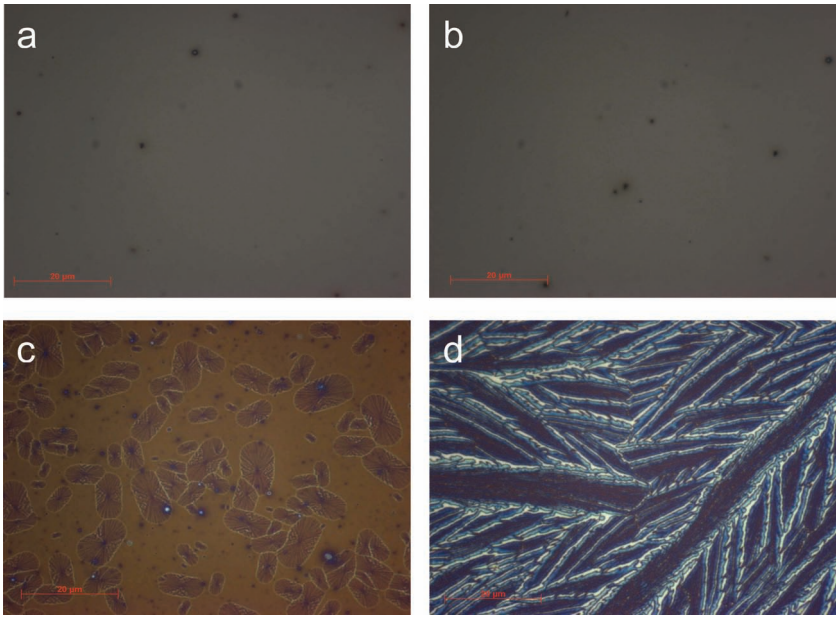

Figure 6. Optical microscopy images of a PCDTBT:$PC_{70}BM$ (1:4) film on a Si/SiOx substrate that are a) as-cast, or annealed for one hour at b) 130 °C, c) 155 °C and d) 200 °C. The scale bar in all images represents 20 µm.

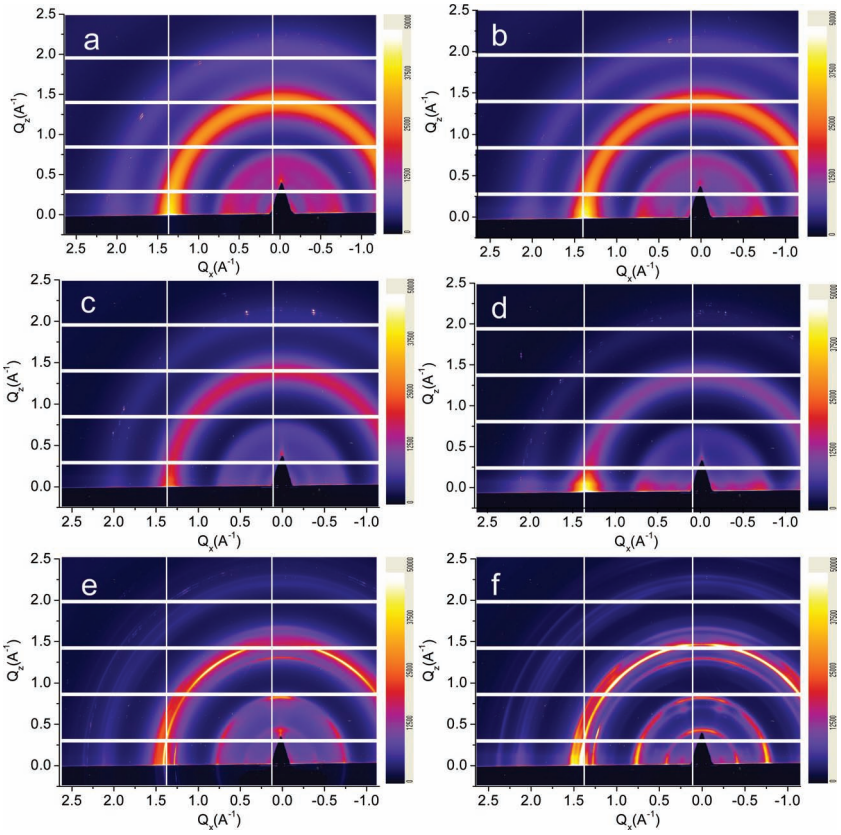

Figure 7. 2D GI-WAXS images of PCDTBT:$PC_{70}BM$ (1:4) films on Si/SiOx substrate recorded from a) an as-cast film, or after annealing at b) 70 °C for 1h, c) 130 °C for 1h, d) 155 °C for 30 minutes, e) 155 °C for 1h and f) 200 °C for 1 h.

To complement our ellipsometry studies, we have used GIWAXS to probe changes in molecular and nanoscale structure in a PCDTBT:$PC_{70}BM$ (1:4) wt% blend thin-film after it has been annealed. **Figure 7**a shows a typical scattering pattern for an as-cast film.[21] It can be seen, that three distinct scattering rings are visible having q-values of 0.67, 1.36, and 2.0 A^{-1}. These broad, diffuse rings correspond to the presence of amorphous (nanoscale) $PC_{70}BM$ domains. Figure 7b, c and d show scattering patterns for similar films that have been annealed at 70 °C and 130 °C for 1 hour and 155 °C for 30 minutes respectively. In all cases we observe a relatively unchanged degree of scattering in the annealed films, indicating the distribution of amorphous $PC_{70}BM$ domains has not been changed significantly by the thermal treatments. To quantify this, we use Scherrer's equation[36] (using a pre-factor of 0.9) to estimate the relative change of the size of $PC_{70}BM$ nanodomains in the blend thin-film, using the full-width-at-half-maximum (FWHM) of the ring at q = 1.36 A^{-1}. This analysis permits us to determine a characteristic length scale for $PC_{70}BM$ nano-domains of 4.2 nm in the as-cast film and 4.6 nm in the films annealed at 130 °C for 1 hour or 155 °C for 30 minutes, suggesting an approximate 10% increase of the $PC_{70}BM$ domain size after the thermal treatment.

Figure 7e shows a scattering pattern of a blend film annealed at 155 °C for 1 hour. Here, a number of sharp rings are apparent that we identify as originating from polycrystalline $PC_{70}BM$. The number and relative intensity of the rings increases in a blend film annealed at 200 °C for 1 hour as shown in Figure 7f. These observations are again consistent with our SE and optical microscopy data, and fully support the notion that partial crystallization of $PC_{70}BM$ only occurs when the film is annealed under these particular conditions.

We can use linear spectroscopy to further probe the conformation and structure of PCDTBT and $PC_{70}BM$ in a PCDTBT:$PC_{70}BM$ blend. Our absorption measurements (data presented in the supporting information, Figure S3, Supporting Information), indicate that the relative absorption of PCDTBT is little changed on blending with $PC_{70}BM$, indicating that no significant modification in conjugation length or conformation occur in the blend, and that ground-state charge transfer does not occur. We observe, however, that the relative photoluminescence intensity of PCDTBT is very efficiently quenched by the presence of the $PC_{70}BM$. We can quantify this by plotting the relative PL intensity emitted by PCDTBT at its peak emission wavelength as a function of $PC_{70}BM$ concentration as shown in **Figure 8**. To demonstrate the efficiency of the PL quenching, we plot the PL intensity emitted at 650 nm from a blend of regio-regular (RR) P3HT and $PC_{70}BM$ blend on the same-scale also as a function of $PC_{70}BM$ concentration. It can be seen that the relative PL intensity from PCDTBT is quenched by two orders of magnitude upon addition of only 9wt% $PC_{70}BM$. Interestingly, at a similar $PC_{70}BM$ concentration, the PL emission intensity

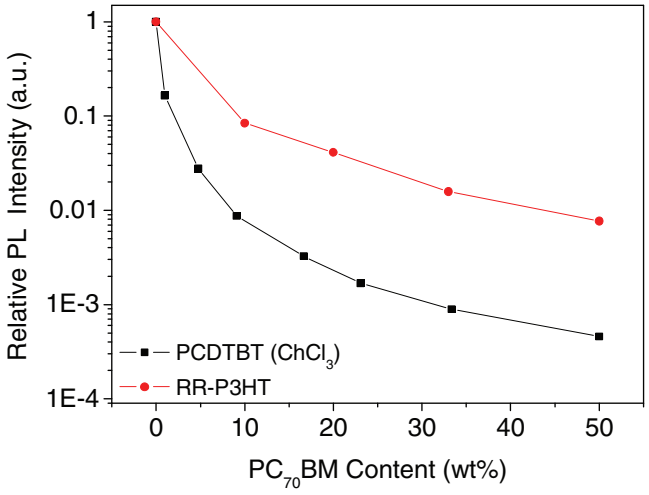

Figure 8. The photoluminescence (PL) intensity determined at the thin-film peak emission wavelength recorded from a blend of PCDTBT:$PC_{70}BM$ (cast from CF) and from RR-P3HT:$PC_{70}BM$ as a function of $PC_{70}BM$ concentration. For both data sets, the emission intensity is normalised to the intensity of a representative pure polymer film.

emitted from the RR-P3HT:$PC_{70}BM$ blend is only quenched by one order of magnitude, indicating the exciton dissociation process in PCDTBT:$PC_{70}BM$ is significantly more efficient than in RR-P3HT:$PC_{70}BM$ blends. We can in fact estimate the typical polymer exciton diffusion length L using the equation $L = L_D(1 - PLQ)^{1/2}$,[37] where PLQ is a relative fraction by which PL emission is quenched with L_D being the exciton diffusion length. For L_D we use a value of 8.5 nm; a value representative of excitons in a typical conjugated polymer.[38] Applying this analysis to the data presented in figure 8, we estimate that L is less than 1 nm in a PCDTBT:$PC_{70}BM$ (e.g. 1:1 wt%) blend thin film. This fine degree of mixing is further evidence for molecular scale miscibility in the PCDTBT:$PC_{70}BM$ blend. We note however that the exciton diffusion length L is anticipated to be much larger in a P3HT:PCBM (e.g. 1:1 wt%) blend thin film, resulting from the existence of relatively larger, phase separated donor and acceptor domains.[39]

In Figure S4 (Supporting Information), we plot PL spectra recorded from PCDTBT:$PC_{70}BM$ blend thin-films containing different amount of $PC_{70}BM$. Here, we observe PL emission at 710 nm when the $PC_{70}BM$ fraction is >50wt%; a wavelength corresponding to singlet emission from $PC_{70}BM$.[40] This suggests that at such high concentrations, a fraction of photogenerated excitons residing on $PC_{70}BM$ cannot undergo diffusion to a PCDTBT molecule within their lifetime to undergo dissociation. This suggests that at this relative $PC_{70}BM$ fraction, $PC_{70}BM$ domains are formed whose size must be commensurate with the exciton diffusion length in $PC_{70}BM$ (which in PCBM has been estimated to be of the order of 5 nm[41]). This observation is consistent with empirical device studies that demonstrate that in this blend system, a $PC_{70}BM$ wt% of at least 50% is needed to allow the formation of pure, interconnected, fullerene domains that permit the efficient extraction of photogenerated charge.

Finally we investigate the role of the blend morphology on hole mobility. Here, we estimate the relative hole mobility from a measurement of the space-charge limited current (SCLC) of thin films using the device architecture ITO/PEDOT:PSS/active layer/Au at room temperature. In **Figure 9**a, we plot hole mobility in a PCDTBT:$PC_{70}BM$ blend as a function of $PC_{70}BM$ concentration. This data was obtained by fitting the J–V curves shown in Figure S5 (Supporting Information) over the range $5 < V < 9$. It can be seen that hole mobility increases with increasing wt% of $PC_{70}BM$. Indeed, we find an 8 times increase in the hole mobility in a 1:4 wt% PCDTBT:$PC_{70}BM$ blend compared to the pure polymer PCDTBT, with mobility increasing from 4×10^{-6} cm^2/Vs to 3.5×10^{-5} cm^2/Vs. This trend is in qualitative agreement with the findings of Cates et al. who measured the SCLC hole mobility for a number of amorphous polymer:functionalized fullerene blends,[42] with improvements in hole mobility by up to 10^3 times measured for a number of amorphous polymer:fullerene systems. The mechanism for this improvement in hole mobility was suggested to result from a general intercalation between the fullerene and the polymer side chains, which inhibits the coiling of the polymer chains and therefore increases the conjugation length and hole mobility. Clearly a significantly smaller increase in hole mobility is observed here on blending PCDTBT with $PC_{70}BM$; the origin of which is not presently clear.

Upon annealing, we find that the hole mobility in devices based on a number of blend compositions is reduced relative to the untreated devices. This can be seen in Figure 9b, where we plot the hole-mobility of a blend of PCDTBT: $PC_{70}BM$ at blend ratios of 1:1, 1:2 and 1:4. We find that in all blend ratios, hole-mobility reduces after the film has been annealed above a temperature of around 70 °C for 30 minutes. We speculate that this reduction in mobility correlates with an increase in disorder within the blend that occurs before the onset of coarse phase separation and crystallization of $PC_{70}BM$. Our GIWAXS measurements confirm (see Figure 3) that π–π stacking in a PCDTBT film is reduced when annealed at a temperature of around 100 °C. The reduced T_g of the blends after thermal annealing (see Figure 2) also indicates that the degree of intermolecular interaction, which is also dependent on π–π stacking between PCDTBT molecules, also undergoes a reduction on annealing. Other work has also suggested that the energetic width of transport states in a PCDTBT film increases on annealing;[22] an effect that results in additional recombination and thus reduced power conversion efficiency for PCDTBT based bulk hetero-junction solar cells. We note that thermal annealing at a relatively low temperature[14,19] may be beneficial to device performance, as this results in the removal of trapped casting solvent which is known to reduce device efficiency. A review of recent literature of PCDTBT based OPVs suggests that this step is not universally adopted, indicating that low temperature "annealing" may be of relatively limited benefit (see Supporting Information Figure S6 & Table S1). We conclude, therefore, that under the annealing protocols explored here, thermal annealing a PCDTBT: $PC_{70}BM$ OPV device at a temperature above ~100 °C results in reduced π–π stacking, reduced hole-carrier mobility and concomitantly reduced device efficiency. When devices are annealed at a temperature in excess of 155 °C, our measurements demonstrate that coarse phase separation occurs between the PCDTBT and the $PC_{70}BM$; an effect that results in a further reduction in device efficiency as the volume density of interfaces at which exciton dissociation occurs is reduced. We believe that other effects will also be important in determining the effectiveness of thermal

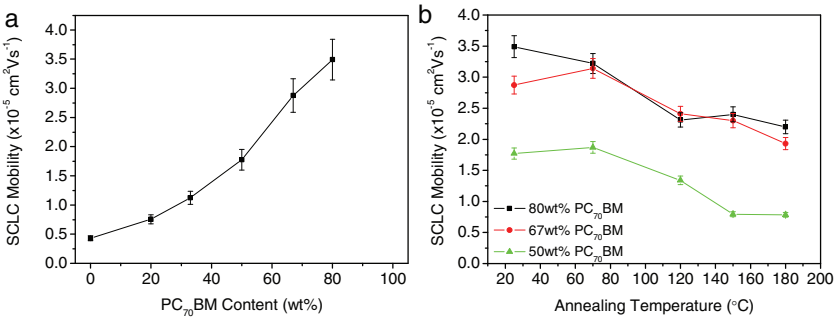

Figure 9. a) A plot of the space-charge limited conduction (SCLC) hole mobility determined from a device based on ITO/PEDOT:PSS/PCDTBT:$PC_{70}BM$/Au as a function of $PC_{70}BM$ concentration. b) The SCLC hole-carrier mobility of PCDTBT:$PC_{70}BM$ blend thin-film device as a function of annealing temperature (annealing time of 30 minutes).

annealing on PCDTBT:PCBM OPV devices. For example, previous work on P3HT:PCBM blends has evidenced diffusion of PCBM into amorphous P3HT.[43] Our previous work[21] has demonstrated that a spin-cast PCDTBT:PCBM blend is characterised by a PCBM-rich surface layer. It is likely therefore that thermal annealing will cause the PCBM to undergo diffusion into the underlying layer that is (compared to the surface), richer in PCDTBT. This would reduce the concentration of PCBM at the film surface and may well reduce the efficiency of charge extraction at the cathode interface. Further work is needed to unravel the importance of such effects.

3. Conclusions

We have investigated the thermal, structural, optical and hole transport properties of the polymer PCDTBT and PCDTBT:$PC_{70}BM$ blend thin-films in order to develop an understanding of this photovoltaic-applicable system. We find that the casting solvent and substrate on which a thin-film blend is deposited modify its glass transition temperature by directing the intermolecular arrangement (π–π stacking) of PCDTBT. Our measurements indicate that coarse phase-separation occurs in a PCDTBT and $PC_{70}BM$ film when it is annealed at a temperature above 155 °C, a point at which the $PC_{70}BM$ undergoes cold-crystallization. Notably however we observe that there is a relatively slow onset of coarse phase separation in the blend, suggesting that these materials are highly miscible. Our device measurements demonstrate that the transport of holes is improved upon addition of $PC_{70}BM$ to a blend, however hole-mobility and device efficiency are found to reduce upon thermal annealing at moderate temperatures (≥100 °C). We associate this reduced device efficiency with an increase in nanoscale structural disorder (a reduction in π–π stacking) that occurs before the onset of coarse $PC_{70}BM$ phase separation. We believe therefore that a PCDTBT:$PC_{70}BM$ blend is an example of a photovoltaic-material system in which efforts to maximize the power conversion efficiency of OPVs should focus on optimizing the composition of the casting solution, film deposition conditions, optical-properties and electrode-composition, as the thermal treatment methodology explored here indicates that this process (apart from the removal of trapped casting solvent) is of limited benefit.

4. Experimental Section

PCDTBT was synthesized according to a previous report[44] and had an M_w of 22.5 kDa, 29.3 kDa and 32.6 kDa and a polydispersity of 1.45, 1.57 and 1.45 respectively as measured by GPC. Unless specifically stated, all measurements were performed on PCDTBT materials having a molecular weight of 32.6 kDa. To prepare thin films, PCDTBT was dissolved in chloroform (CF) or dichlorobenzene (DCB) at 4 mg/mL, and then passed through a 0.45μm filter and then blended with $PC_{70}BM$ in CF or DCB (at 25 mg/mL) to create a PCDTBT:$PC_{70}BM$ blend solution. The solutions were spin-cast on a Si/SiOx substrate (a Si wafer having a 1.8 nm surface a layer of SiOx) or Si/SiOx covered with a 30 nm thick layer of PEDOT:PSS.

Spectroscopic ellipsometry (using a M2000v, J.A. Woollam Co. ellipsometer) was used to determine film thickness at room temperature, employing a Cauchy model[45] to fit Ψ (the ratio of the amplitude of the incident and reflected light beams) and Δ (the ratio of the phase lag of the incident and reflected light beams) over the wavelength range in which the film is optically transparent (750 to 1000 nm).

Spectroscopic ellipsometry was also used to characterise T_g of the PCDTBT:$PC_{70}BM$ blends as they were annealed. For measurement, thin films deposited on a substrate were put on a Linkam heating/cooling stage within a cell containing a N_2 atmosphere. The cell has two transparent windows to allow transmission of the polarized incident and reflected ellipsometry beams. The films were heated from 25 to 200 °C under a N_2 atmosphere and then cooled to 25 °C at a rate of 5 °C min^{-1}. During the heating and cooling cycles, Ψ and Δ were recorded, with a change in slope of Ψ vs temperature being used to identify T_g.

Phase separation in PCDTBT:$PC_{70}BM$ blends (cast from CF) during thermal annealing was characterized using spectroscopic ellipsometry. During the annealing cycle, films were heated toward the desired annealing temperature at 90 °C min^{-1} (the fastest heating rate that can be delivered by the Linkam stage). This process approximates the procedure that is used when a device is placed onto a hot plate for thermal annealing. The temperature fluctuation of the Linkam stage during the isothermal annealing process is estimated to be ±0.1 °C. Samples were held at constant temperature (130, 150, 155 and 200 °C) for 1 hour and then cooled to room temperature (approximately 25 °C) at 90 °C min^{-1}.

Grazing incidence wide angle scattering was conducted at the I16 beamline, at the Diamond Light Source, UK. A custom sample cell with a Kapton exit window was constructed to surround the sample with helium in order to minimise air scatter. The vertical blade above the sample remove scatter not associated with the sample, and an internal beamstop interceted the direct and reflected beams before the Kapton window. GI-WAXS scattering patterns were recorded using 12 keV energy X-rays and a Pilatus 2M detector to record images with a 30 second exposure time.

Photoluminescence (PL) spectra from blend films were recorded using a Horiba Fluoromax spectrometer under a fixed excitation and detection geometry. PL spectra were acquired following excitation at 400 nm and were corrected for thin-film absorption effects.

To fabricate OPV devices, ITO/glass substrates were cleaned by sonication in dilute NaOH and then in IPA. A 30 nm PEDOT:PSS (Baytron 4083 Special Grade) anode layer was then spin cast in air on the ITO/glass substrate. The substrates were transferred to a nitrogen filled glove box. The PEDOT:PSS films were annealed for one minute at 110 °C to fully dry the PEDOT:PSS layer after which a PCDTBT:$PC_{70}BM$ layer was cast onto the anode forming a 70 nm thick film. Following this, a 100 nm thick aluminum cathode was deposited onto the film surface using a thermal evaporator. The devices were then thermally annealed at various temperatures for 30 minutes. Devices were finally encapsulated using a glass slide and epoxy glue before testing. PCEs were determined using a Lot Oriel 91159 AM 1.5G solar simulator controlled using a Keithley 237 source measure unit. An NREL calibrated silicon cell was used to calibrate the power output to 100mW cm^{-2} at 25°C. Space charge limited conduction mobility values were calculated from dark J-V measurements on ITO/PEDOT:PSS/active layer/Au devices after correction for the device built-in voltage.

Supporting Information

Supporting Information is available from the Wiley Online Library or from the author.

Acknowledgements

We thank financial support from EPSRC via grant "Optimization of polymer photovoltaic devices through control of phase separation" (Grant reference EP/F016433/1). A.J.P. acknowledges an award of an EPSRC DTA PhD studentship. Supporting Information is available online from Wiley InterScience or from the author. We thank Diamond Light

Source via a program grant MT1203 for the grazing incidence X-ray scattering experiment and Dr. Gareth Nisbet for beam line assistance.

Received: October 18, 2011
Revised: November 29, 2011
Published online: February 6, 2012

[1] S. Günes, H. Neugebauer, N. S. Sariciftci, *Chem. Rev.* **2007**, *107*, 1324.
[2] G. Dennler, M. C. Scharber, C. J. Brabec, *Adv. Mater.* **2009**, *21*, 1323.
[3] C. J. Brabec, S. Gowrisanker, J. J. M. Halls, D. Laird, S. J. Jia, S. P. Williams, *Adv. Mater.* **2010**, *22*, 3839.
[4] Z. C. He, C. M. Zhong, X. Huang, W.-Y. Wong, H. B. Wu, L. W. Chen, S. J. Su, Y. Cao, *Adv. Mater.* **2011**, *23*, 4636.
[5] W. L. Ma, C. Y. Yang, X. Gong, K. Lee, A. J. Heeger, *Adv. Funct. Mater.* **2005**, *15*, 1617.
[6] X. Yang, J. Loos, S. C. Veenstra, W. J. H. Verhees, M. M. Wienk, J. M. Kroon, M. A. J. Michels, R. A. J. Janssen, *Nano Lett.* **2005**, *5*, 579.
[7] M. Campoy-Quiles, T. Ferenczi, T. Agostinelli, P. G. Etchegoin, Y. Kim, T. D. Anthopoulos, P. N. Stavrinou, D. D. C. Bradley, J. Nelson, *Nat. Mater.* **2008**, *7*, 158.
[8] D. Chen, A.Nakahara, D. G. Wei, D.Nordlund, T. P. Russell, *Nano Lett.* **2011**, *11*, 561.
[9] T. Wang, A. D. F. Dunbar, P. A. Staniec, A. J. Pearson, P. E. Hopkison, J. E. Macdonald, S. Lilliu, C. Pizzey, N. J. Terrill, A. M. Donald, A. J. Ryan, R. A. L. Jones, D. G. Lidzey, *Soft Matter* **2010**, *6*, 4128.
[10] A. J. Moule, K. Meerholz, *Adv. Mater.* **2008**, *20*, 240.
[11] T. Wang, A. J. Pearson, D. G. Lidzey, R. A. L. Jones, *Adv. Funct. Mater.* **2011**, *21*, 1383.
[12] Y. Zhao, Z. Xie, Y. Qu, Y. Geng, L. Wang, *Appl. Phys. Lett.* **2007**, *90*, 043504.
[13] G. Li, Y. Yao, H. Yang, V. Shrotriya, G. Yang, Y. Yang, *Adv. Funct. Mater.* **2007**, *17*, 1636.
[14] A. J. Parnell, A. D. F. Dunbar, A. J. Pearson, P. A. Staniec, A. J. C. Dennison, H. Hamamatsu, M. W. A. Skoda, D. G. Lidzey, R. A. L. Jones, *Adv. Mater.* **2010**, *22*, 2444.
[15] T. Erb, U. Zhokhavets, G. Gobsch, S. Raleva, B. Stühn, P. Schilinsky, C. Waldauf, C. J. Brabec, *Adv. Funct. Mater.* **2005**, *15*, 1193.
[16] T. M. Clarke, A. M. Ballantyne, J. Nelson, D. D. C. Bradley, J. R. Durrant, *Adv. Funct. Mater.* **2008**, *18*, 4029.
[17] R. A. Marsh, J. M. Hodgkiss, S. Albert-Seifried, R. H. Friend, *Nano Lett.* **2010**, *10*, 923.
[18] V. D. Mihailetchi, H. X. Xie, B. de Boer, L. J. A. Koster, P. W. M. Blom, *Adv. Funct. Mater.* **2006**, *16*, 699.
[19] S. H. Park, A. Roy, S. Beaupré, S. Cho, N. Coates, J. S. Moon, D. Moses, M. Leclerc, K. Lee, A. J. Heeger, *Nat. Photonics* **2009**, *3*, 297.
[20] T.-Y. Chu, S. Alem, S.-W. Tsang, S.-C. Tse, S. Wakim, J. Lu, G. Dennler, D. Waller, R. Gaudiana, Y. Tao, *Appl. Phys. Lett.* **2011**, *98*, 253301.
[21] P. A. Staniec, A. J. Parnell, A. D. F. Dunbar, H. Yi, A. J. Pearson, T. Wang, P. E. Hopkinson, C. Kinane, R. M. Dalgliesh, A. M. Donald, A. J. Ryan, A. Iraqi, R. A. L. Jones, D.G. Lidzey, *Adv. Energy Mater.* **2011**, *1*, 499.
[22] Z. M. Beiley, E. T. Hoke, R. Noriega, J. Dacuna, G. F. Burkhard, J. A. Bartelt, A. Salleo, M. F. Toney, M. D. McGehee, *Adv. Energy Mater.* **2011**, *1*, 954.
[23] A. J. Pearson, P. E. Hopkinson, T. Wang, P. A. Staniec, R. A. L. Jones, A. M. Donald, D. G. Lidzey, *Macromolecules* **2012**, DOI: 10.1021/ma202063k.
[24] J. L. Keddie, R. A. L. Jones, R. A. Cory, *Europhys. Lett.* **1994**, *27*, 59.
[25] C. Müller, J. Bergqvist, K. Vandewal, K. Tvingstedt, A. S. Anselmo, R. Magnusson, M. I. Alonso, E. Moons, H. Arwin, M. Campoy-Quiles, O. Inganäs, *J. Mater. Chem.* **2011**, *21*, 10676.
[26] G. Reiter, P. G. de Gennes, *Eur. Phys. J. E* **2001**, *6*, 25.
[27] L. Chang, H. W. A. Lademann, J.-B. Bonekamp, K. Meerholz, A. J. Moulé, *Adv. Funct. Mater.* **2011**, *21*, 1779.
[28] T. Wang, A. J. Pearson, A. D. F. Dunbar, P. A. Staniec, D. C. Watters, D. Coles, H. Yi, A. Iraqi, D. G. Lidzey, R. A. L. Jones, Unpublished.
[29] P. Rittigstein, R. D. Priestley, L. J. Broadbelt, J. M. Torkelson, *Nat. Mater.* **2007**, *6*, 278.
[30] D. H. Wang, J. S. Moon, J. Seifter, J. Jo, J. H. Park, O. O. Park, A. J. Heeger, *Nano Lett.* **2011**, *11*, 3163.
[31] J. A. Forrest, K. Dalnoki-Veress, J. R. Stevens, J. R. Dutcher, *Phys. Rev. Lett.* **1996**, *77*, 2002.
[32] P. E. Hopkison, P. A. Staniec, A. J. Pearson, A. D. F. Dunbar, T. Wang, A. J. Ryan, R. A. L. Jones, D. G. Lidzey, A. M. Donald. *Macromolecules* **2011**, *44*, 2908.
[33] J. M. Hutchinson, *Prog. Polym. Sci.* **1995**, *20*, 703.
[34] H. Richardson, Í. López-García, M. Sferrazza, J. L. Keddie, *Phys. Rev. E* **2004**, *70*, 051805.
[35] S. Kawana, R. A. L. Jones, *Eur. Phys. J. E* **2003**, *10*, 223.
[36] A. Patterson, *Phys. Rev.* **1939**, *56*, 978.
[37] F. C. Jamieson, E. B. Domingo, T. McCarthy-Ward, M. Heeney, N. Stingelin, J. R. Durrant, *Chem. Sci.* **2012**, *3*, 485.
[38] P. E. Shaw, A. Ruseckas, I. S. W. Samuel, *Adv. Mater.* **2008**, *20*, 3516.
[39] A. J. Pearson, S. A. Boden, D. M. Bagnall, D. G. Lidzey, C. Rodenburg. *Nano Lett.* **2011**, *11*, 4275.
[40] M. Moranaet al. *Adv. Funct. Mater.* **2010**, *20*, 1180.
[41] S. Cook, A. Furube, R. Katoh, L. Han, *Chem. Phys. Lett.* **2009**, *478*, 33.
[42] N. C. Cates, R. Gysel, J. E. P. Dahl, A. Sellinger, M. D. McGehee, *Chem. Mater.* **2010**, *22*, 3543.
[43] N. D. Treat, M. A. Brady, G. Smith, M. F. Toney, E. J. Kramer, C. J. Hawker, M. L. Chabinyc, *Adv. Energy Mater.* **2011**, *1*, 82.
[44] N. Blouin, A. Michaud, M. Leclerc, *Adv. Mater.* **2007**, *19*, 2295.
[45] Complete EaseTM Data Analysis Manual, J.A. Woollam Co., Inc. Lincoln, **2008.**